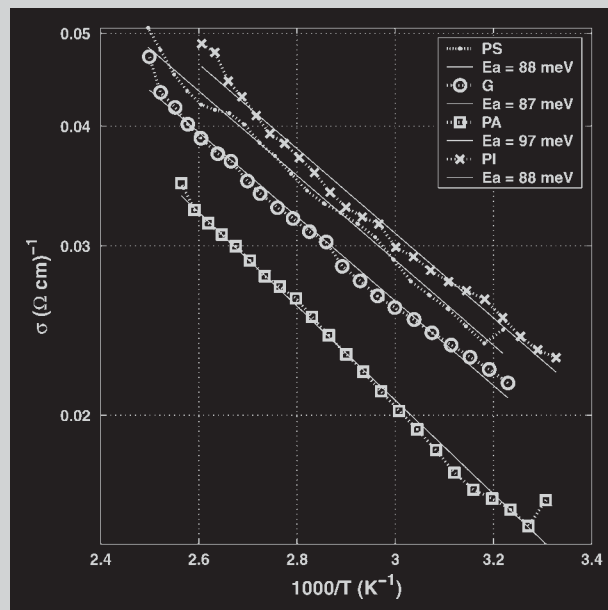


ppap.200500145

**Summary:** Hydrogenated nanocrystalline silicon (nc-Si:H) was deposited by plasma-enhanced chemical vapor deposition (PECVD) on transparent polymers in order to qualify these for possible use as electronic substrates. As a first step, plasma etch experiments in pure H<sub>2</sub> revealed small etch rates for these materials. Thin films of nc-Si:H were then deposited on samples placed on the grounded electrode of a “Reinberg”-type parallel plate RF (13.56 MHz) PECVD reactor, at various substrate temperatures (25 °C ≤ T<sub>s</sub> ≤ 250 °C), using SiH<sub>4</sub> diluted in H<sub>2</sub> as the feed-gas. Thermally induced failure of the nc-Si:H/polymer composite was avoided within a certain range of deposition conditions, permitting structural and electrical characterization of the deposits.

Temperature-dependent conductivity,  $\sigma(T)$ , for nanocrystalline silicon (nc-Si:H) films on glass and three polymer substrates, all deposited at T<sub>s</sub> = 175 °C.



## PECVD of Nanocrystalline Si Layers on High- $T_g$ Polymer Substrates

Luke A. MacQueen,<sup>1</sup> Janik Zikovsky,<sup>1</sup> Gilles Dennler,<sup>2</sup> Mohamed Latreche,<sup>3</sup> Grzegorz Czeremuszkin,<sup>3</sup> Michael R. Wertheimer\*<sup>1</sup>

<sup>1</sup>Groupe des Couches Minces and Department of Engineering Physics, École Polytechnique, Montréal, QC, Canada  
Fax: 001 514 340 3218; E-mail: michel.wertheimer@polymtl.ca

<sup>2</sup>Linz Institute for Organic Solar Cells (LIOS), Johannes Kepler University, Linz, Austria

<sup>3</sup>Nova-Plasma Inc., Montréal, QC, Canada

Received: October 7, 2005; Revised: November 25, 2005; Accepted: November 29, 2005; DOI: 10.1002/ppap.200500145

**Keywords:** PECVD; nanocrystalline silicon; macroelectronics; flexible electronics; high- $T_g$  plastics; OLED

### Introduction

Electronic devices on flexible polymer substrates are becoming increasingly important, for example in displays, photovoltaic cells, etc. The advantages of using polymer substrates instead of glass for electronic applications include light weight, flexibility and conformability, and low cost with the possibility of roll-to-roll processing (large-area electronics). So far, the adoption of polymers for electronic applications has been slow due to their limited compatibility with semiconductor fabrication processes. In particular, the relatively high linear expansion coefficient,

α, and low glass transition temperature, T<sub>g</sub>, of most polymers limit their use to temperatures below 300 °C. Several high- $T_g$  polymers (220 °C < T<sub>g</sub> < 330 °C) with optical transparency, good chemical resistance and barrier properties have recently been developed for use in organic (OLED) display technology,<sup>[1,2]</sup> and these have motivated the present research.

For many applications, thin film transistor (TFT) matrix arrays are required, for example to drive the individual pixel elements of a display.<sup>[3,4]</sup> Hydrogenated amorphous silicon (a-Si:H) is a low-temperature material which is presently used as a TFT semiconductor, but its inherently low charge

carrier mobility limits the density at which TFTs can be laid out. Better nano-structural control of low-temperature Si films is therefore required to increase TFT density and to reduce operating power of TFT-based devices. Silicon can be deposited as various structural phases ranging between a-Si and the fully crystalline state (c-Si); these include nanocrystalline (nc-Si), microcrystalline ( $\mu$ c-Si), and polycrystalline (pc-Si) materials. The first two (nc-Si and  $\mu$ c-Si) comprise an a-Si matrix in which are dispersed many tiny crystallites (small volumes of c-Si), the “nano” and “micro” prefixes indicating the mean crystallite size. pc-Si refers to a material that is devoid of the amorphous matrix, the crystallites being separated by abrupt grain boundaries. Although c-Si and pc-Si possess high carrier mobility in comparison to a-Si, they are brittle and inflexible, unlike a-Si. Furthermore, as transistor dimensions are reduced, conductivity anisotropy within the pc-Si material becomes problematic.

Nanocrystalline silicon (nc-Si:H) is a preferred semiconductor for fabricating TFTs, and deposition by plasma-enhanced chemical vapor deposition (PECVD) is particularly advantageous when using temperature-sensitive substrate materials. With PECVD, the crystalline volume fraction of as-deposited Si films can be varied between 0 and close to 100% within a useful range of “low” substrate temperatures,  $T_s$ ,<sup>[5–7]</sup> eliminating the requirement of post-deposition laser or thermal annealing. The objective of the present research has, therefore, been to deposit nc-Si:H films at the lowest possible  $T_s$  values, and to characterize their structural and electrical properties. No coatings were deposited before or after the nc-Si:H, which was deposited directly on the various substrates in order to simplify the estimation of stress values induced within the film-substrate (f-s) structure. Such stress values, resulting from differential thermal expansion,  $\alpha$ , can be correlated with results of structural and electrical measurements. In order to reduce possible contamination of the nc-Si:H by unwanted “dopant” elements (C, O, N, etc) arising from substrate ablation (etching) during PECVD, we first performed etching experiments in order to identify the optimal conditions for high-quality nc-Si:H film growth.

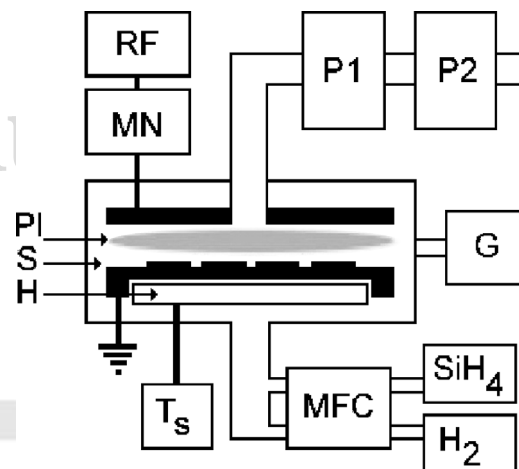


Figure 1. Schematic of RF-PECVD system: RF: 13.56 MHz Power Supply; MN: Matching Network; P1: Turbo Molecular Pump; P2: Rotary Pump; G: Pressure Gauge;  $T_s$ : Temperature Control; MFC: Mass Flow Control; Pl: Plasma; S: Substrates; H: Heater.

## Experimental Part

### Etching and Deposition Experiments

Etching and deposition experiments were performed in a “Reinberg-type” parallel-plate RF-PECVD reactor, operating at 13.56 MHz (Figure 1). The ranges of operating parameters selected and the reasons for these choices will be clarified later in this text. The substrate materials used in this research and some of their key properties for this work ( $\alpha$  and  $T_g$ ) are presented in Table 1. Since nc-Si:H films must not be contaminated by unwanted impurities, the polymer substrates must be resistant towards ablation (etching) in  $H_2$ -rich plasma during the PECVD process. It was, therefore, deemed necessary to investigate possible etching of the polymer substrates as a preliminary step. Etch rates were determined by partially masking the substrates with 50 nm Au layers before exposing them to  $H_2$  plasma at various RF power densities ( $50 \text{ mW/cm}^2 < P < 500 \text{ mW/cm}^2$ ), and then profiling the etched areas by Atomic Force Microscopy (AFM). Such experiments were carried out with the substrates on the

Table 1. Properties of the substrate materials investigated.

| Substrate                                   | Source/Manufacturer <sup>[2]</sup> | Symbol | $T_g$ ( $^{\circ}\text{C}$ ) | $\alpha$<br>ppm/ $^{\circ}\text{C}^{\text{a}}$ |
|---|------------------------------------|--------|------------------------------|--|
| APPEAR <sup>®</sup> (cyclic polyolefin)     | Promerus LLC                       | PO     | 330                          | $60 + T/4$                                     |
| ARYLITE <sup>®</sup> (polyarylate)          | Ferrania Imaging Technologies.     | PA     | 325                          | $50 + T/15$                                    |
| SUMILITE <sup>®</sup> [poly(ether sulfone)] | Sumitomo Bakelite Co. Ltd.         | PS     | 223                          | $50 + T/14$                                    |
| KAPTON <sup>®</sup> (polyimide)             | DuPont de Nemours & Co.            | PI     | 360                          | 20   |
| Glass (Corning 2947)                        | Corning Inc.                       | G      | —                            | 9  |

<sup>a)</sup>  $T$ -dependent  $\alpha$  values are linear approximations of data from ref.<sup>[1]</sup>

grounded or powered electrodes. The above-noted variation in  $P$  was then repeated, this time with a certain fixed concentration,  $C_{\text{SiH}_4}$ , of  $\text{SiH}_4$  added to the  $\text{H}_2$  ( $\text{SiH}_4$  concentration,  $C_{\text{SiH}_4} = [\text{SiH}_4]/([\text{SiH}_4] + [\text{H}_2]) = 6.25\%$ ). The resulting a-Si:H films were used for comparing deposition rates to etch rates.

In the case of nc-Si:H deposition experiments,  $P$  was maintained at  $50 \text{ mW/cm}^2$ , with substrates placed on the grounded electrode only. The  $\text{SiH}_4$  and  $\text{H}_2$  partial pressures were maintained constant at 8 mTorr and 120 mTorr, respectively ( $C_{\text{SiH}_4} = 6.25\%$ ), the chamber pressure was always  $p = 150 \text{ mTorr}$  (20 Pa), while the substrate temperature,  $T_s$ , was varied between  $25^\circ\text{C}$  and  $250^\circ\text{C}$ . Typical deposition durations were 200 min, and film thicknesses,  $d_f$ , measured by variable angle spectroscopic ellipsometry (VASE, J. Woollam & Co.), were  $120 \pm 15 \text{ nm}$ .

### Differential Thermal Expansion

The maximum value of  $T_s$  at which we could deposit nc-Si:H films on the substrates listed in Table 1 was mainly limited by the differences in thermal expansion coefficients,  $\alpha$ , of the deposited Si films,  $\alpha_f$ , and the substrates,  $\alpha_s$  (see Figure 2 and Table 1). Substrates were heated ( $dT_s/dt \approx 1^\circ\text{C/min}$ ) and held at the selected value of  $T_s$  for 30 min prior to film deposition. Precautions were taken to limit the amount of structural relaxation (for example, buckling or rolling) of the film-substrate (f-s) composite during deposition, and the PECVD chamber was gradually returned to ambient conditions ( $dT_s/dt \approx -1^\circ\text{C/min}$ ) after the deposition had terminated. The differential thermal strain between the substrates and the film deposits can be approximated by

$$\delta = (\alpha_s - \alpha_f)\Delta T, \quad (1)$$

where  $\alpha_s$  and  $\alpha_f$  are the respective coefficients of thermal expansion. The thicknesses,  $d_f$ , of our nc-Si:H deposits were typically at least a thousand times less than those of the substrates. When  $d_s/d_f \approx 10^3$  such as in the present case, curvature of the f-s composite resulting from stress relaxation may be expected to obey the Stoney formula up to  $Y_f/Y_s \approx 100$ , where  $Y$  is Young's modulus,<sup>[18]</sup> in the present case  $Y_f \approx 150\text{--}200 \text{ GPa}$ <sup>[9]</sup> and  $1.9 < Y_s < 5 \text{ GPa}$ .<sup>[11]</sup> Since  $d_s Y_s/d_f Y_f > 10$ , we can use the

following expression to estimate the compressive stress in the film due to differential thermal contraction:<sup>[10]</sup>

$$s_f = \frac{Y_f \delta}{(1 - \nu_f)} \quad (2)$$

where  $\nu_f$  is Poisson's ratio of nc-Si:H. Films deposited on PO, the polymer with by far the highest  $\alpha_s$  value (see Figure 2 and Table 1), were observed to delaminate at  $T_s \geq 200^\circ\text{C}$ ; in this particular case, the compressive strain  $\alpha_s \Delta T \approx 1.7\%$  resulted in a stress  $s_f \approx 3.6 \text{ GPa}$ , a value that clearly exceeded the f-s interfacial adhesion strength. These may, therefore, be considered the limiting conditions for successful deposition of stable nc-Si:H film coatings.

### Physico-Chemical Characterization of Si Deposits

Thin Si deposits were subjected to both structural and electrical characterizations, primarily by micro-Raman spectroscopy (MRS) and by DC conductivity measurements, respectively. MRS was used to estimate the crystalline volume fractions,  $X_c$ , of the films by comparing the areas under Raman peaks corresponding to the crystalline (c) and amorphous (a) transverse optical lattice vibrations (c-TO and a-TO).<sup>[11–17]</sup> We used an argon-ion laser,  $\lambda = 514 \text{ nm}$ , in the Stokes configuration, and calibrated the measured spectra with a c-Si sample displaying a c-TO peak centered at  $520.5 \text{ cm}^{-1}$  with a full width at half-maximum (FWHM) of  $3.886 \text{ cm}^{-1}$ . Data analysis (spectral deconvolution and area integration) was done using BOMEM GRAMS/32 software (Galactic Industries Co., Salem, NH).

DC conductivity measurements were performed by the four-point-probe method,<sup>[18]</sup> with samples mounted on a temperature-controlled substrate holder and using computerized data acquisition. This system, that allowed us to measure sheet conductivity during repeated thermal cycling, comprised a Keithley 220 programmable current source, an Agilent 34401A multimeter, and a Tempron temperature controller; probe tip spacings and radii were  $1.59 \text{ mm}$  and  $17.8 \mu\text{m}$ , respectively. For the case of very low conductivity samples ( $\sigma < 10^{-6} \text{ S/cm}$ ), planar aluminum electrodes (with a  $100 \mu\text{m}$  gap) were evaporated on the Si films, and measurements were carried out under vacuum.

## Results and Discussion

### Etching and Deposition Experiments

Figure 3 presents etch rates,  $E$ , of three of the present polymers in pure  $\text{H}_2$  plasma, samples being placed either on the grounded or the powered electrodes. Significantly higher etch rates are seen to occur on the powered electrode ( $P < 0$ , in Figure 3) on account of d.c.-bias induced ion bombardment.<sup>[19]</sup>  $E$  values were very small for the case of low power densities ( $|P| < 50 \text{ mW/cm}^2$ ), especially in the absence of energetic ion bombardment, on the grounded electrode. Figure 4 presents the influence of  $P$  on the deposition rate,  $D$ , and the refractive index,  $n$ , of a-Si:H films, deposited at  $T_s = 27^\circ\text{C}$  on glass. Dense films (high

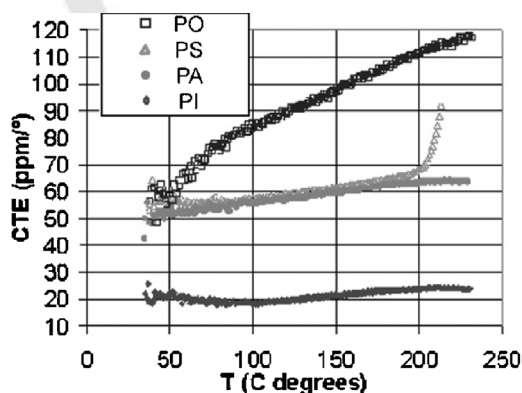


Figure 2. Coefficient of thermal expansion,  $\alpha$ , ( $\text{ppm}/^\circ\text{C}$ ) of four high- $T_g$  polymers versus  $T$ . From ref.,<sup>[11]</sup> with permission.

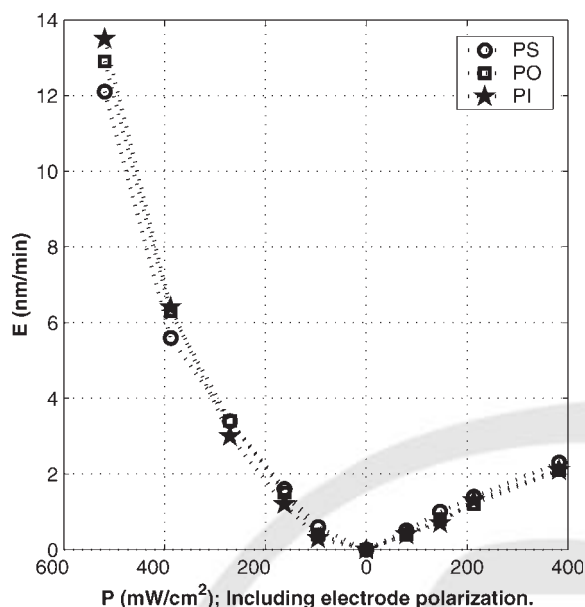


Figure 3. Etch rates,  $E$ , for three of the high- $T_g$  polymers, as a function of power density,  $P$ .  $P < 0$  refers to substrates placed on the powered electrode.

$n$  values) with low concentrations of voids and other defects are produced in the low- $P$  (low- $D$ ) regime, substrates being placed on the grounded electrode.

### Raman Spectroscopy

Micro-Raman spectroscopy (MRS) is a non-destructive optical technique that can be used to analyze structural

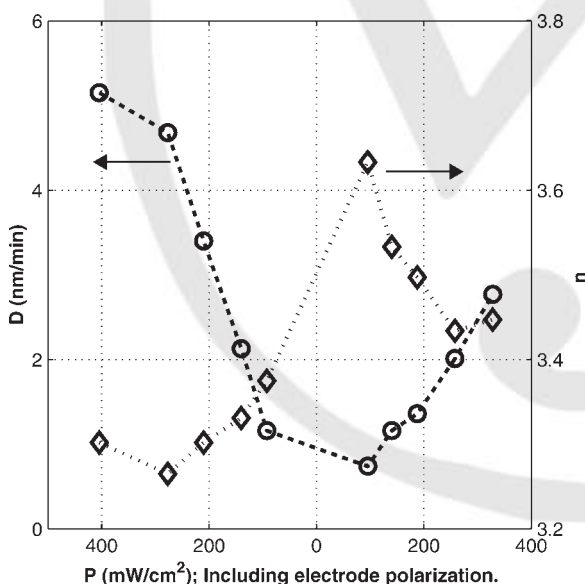


Figure 4. Influence of power density,  $P$ , on deposition rate,  $D$ , and refractive index,  $n$ , of a-Si:H films, deposited on glass at  $T_s = 27^\circ\text{C}$ .  $P < 0$  refers to substrates placed on the powered electrode.

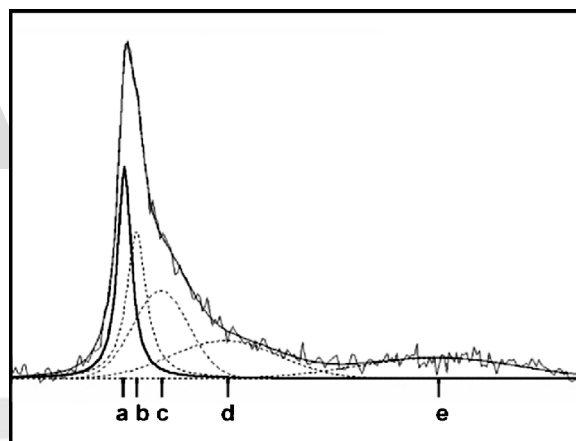


Figure 5. Example of a Si-Si micro-Raman spectrum, corresponding to an nc-Si:H film deposited on PA at  $T_s = 175^\circ\text{C}$  (see Table 2 for description).

properties of semiconductors.<sup>[6,11–17]</sup> In silicon, the transverse optical (TO) vibration modes differ between c-Si and a-Si:H materials. Within a multiphase material, for example nc-Si:H, we can estimate the crystalline volume fraction,  $X_c$ , by comparing the contributions from the “c” and “a” peaks. Further information can also be derived from the center frequency positions,  $\omega$ , and the full widths at half-maximum (FWHM),  $\Gamma$ , of the peaks, as will be discussed below.  $X_c$  can be estimated using the formula:<sup>[11]</sup>

$$X_c = \frac{I_c + I_{gb}}{I_c + I_{gb} + y(L)I_a} \quad (3)$$

where  $I_c$ ,  $I_{gb}$ , and  $I_a$  are the integrated intensities of (or areas under) the “crystalline”, intermediate (grain boundary), and “amorphous” peaks, respectively (see Figure 5 and Table 2). The weighting function,  $y(L)$ , is the ratio of the scattering cross-section of c-Si to a-Si:H, which depends on the excitation wavelength,  $\lambda$ , and the grain size,  $L$ ; according to Bustarret et al.,<sup>[11]</sup>  $y(L) = 0.1 + \exp(-L/250)$ ; in other words,  $y$  is close to unity,  $0.9 < y(L) < 1.1$  for the case of small grain sizes ( $0 < L < 20$  nm). Since the deposition conditions used here are known to lead to  $L$  values  $< 20$  nm,<sup>[5–7]</sup> we have used  $y = 1$  in our calculations,

Table 2. Data analysis of the micro-Raman spectrum shown in Figure 5.

| Symbol | $\omega_0$<br>cm <sup>-1</sup> | $\Gamma$<br>cm <sup>-1</sup> | Peak assignment | Reference |
|--------|--------------------------------|------------------------------|-----------------|-----------|
| a      | 520                            | 4–15                         | c-Si TO         | [6,11–17] |
| b      | 494–510                        | 20–30                        | gb-Si           | [6,12,13] |
| c      | 480                            | 45–80                        | a-Si:H TO       | [6,11–17] |
| d      | 440                            | ≈100                         | a-Si:H LO       | [17]      |
| e      | 330                            | ≈120                         | a-Si:H LA       | [17]      |

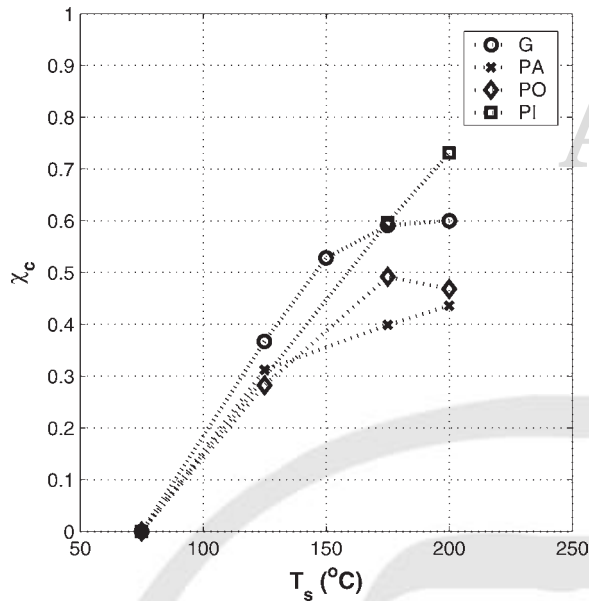


Figure 6<sup>Q1</sup>. The influence of  $T_s$  on the crystalline volume fraction,  $X_c$ , estimated using Equation (3), for different substrate materials.

the results of which appear in Figure 6. Figure 6 represents a plot of  $X_c$  vs.  $T_s$ : films are seen to be essentially amorphous ( $X_c \approx 0$ ) for  $T_s < 100^\circ\text{C}$ , but the crystalline fraction,  $X_c$ , then rises near-linearly with increasing  $T_s$  values. The majority of our nc-Si:H films, corresponding to deposits made at  $150^\circ\text{C} \leq T_s \leq 225^\circ\text{C}$ , show a maximum  $X_c$  of  $\approx 0.5$ . Increasing either  $T_s$  or the deposition duration (film thickness) resulted in unstable film-substrate composite structures, as will be discussed later.

The measured peak-center positions,  $\omega$ , and FWHM,  $\Gamma$ , of our a-Si:H and nc-Si:H samples vary considerably, depending on the chosen substrate material and  $T_s$ . For the c-TO peak  $\omega = 516 \pm 4 \text{ cm}^{-1}$  and  $\Gamma = 13 \pm 3 \text{ cm}^{-1}$ , while for the a-TO peak  $\omega = 485 \pm 10 \text{ cm}^{-1}$  and  $\Gamma = 55 \pm 10 \text{ cm}^{-1}$ . Onset of the intermediate peak (Table 2, symbol b) coincided with that of the crystalline peak; its  $\omega$  and  $\Gamma$  values were  $\omega = 503 \pm 4 \text{ cm}^{-1}$  and  $\Gamma = 25 \pm 5 \text{ cm}^{-1}$ . A full examination of this data will not be presented here due to the many film properties and measurement conditions that can affect  $\omega$  and  $\Gamma$ . Some of these factors include: (i) the size and shape of crystallites,<sup>[14]</sup> (ii) the local temperature of the measured volume,  $T_m$ ,<sup>[15]</sup> which can be raised by the probe laser, and (iii) residual stresses (both intrinsic and extrinsic) which are variable throughout the film thickness.<sup>[16]</sup>

### DC Conductivity

The electrical conductivity of semiconducting materials such as nc-Si:H,  $\sigma(T)$ , is thermally activated and therefore

obeys the Arrhenius relation:

$$\sigma(T) = \sigma_0 \exp\left(\frac{-E_a}{kT}\right) \quad (4)$$

where  $\sigma_0$  is the pre-exponential factor,  $E_a$  is the so-called activation energy, and  $k$  is Boltzmann's constant. For the case of nc-Si:H films grown directly on plastic substrates, the temperature dependence of  $\sigma(T)$  is also influenced by stress in the film resulting from the differential thermal expansion between it and the substrate.<sup>[8–10]</sup> After repeated thermal cycles, excessive stresses may result in failure (cracking and delamination of the nc-Si:H) of the f-s composite. Figure 7 and 8 present  $\sigma(T)$  data for nc-Si:H films on PA and PO substrates, respectively, measured while continuously heating and cooling the composites ( $dT/dt = 0.33^\circ\text{C}/\text{min}$ ) within a range of temperatures,  $40^\circ\text{C} < T < 120^\circ\text{C}$ . “Good” f-s composite structures display the expected near-linear behavior (Figure 7), while a highly non-linear behaviour is observed for the case of nc-Si:H/PO (Figure 8). Values of  $\sigma$  and  $E_a$  for “good” nc-Si:H films grown at particular fixed conditions were always found to be very similar, independent of whether they were deposited on polymers or on glass. “Arrhenius-like” behavior within the specified  $T$  range was observed for all films deposited at  $T_s \leq 175^\circ\text{C}$ , except for those grown on the PO substrate. The reason for this “anomaly” is the following: As shown in Figure 2, APPEAR<sup>®</sup> (PO) undergoes a structural transition at  $T \approx 60^\circ\text{C}$  that gives rise to increasing  $\alpha(T)$  values above that temperature. As a result,

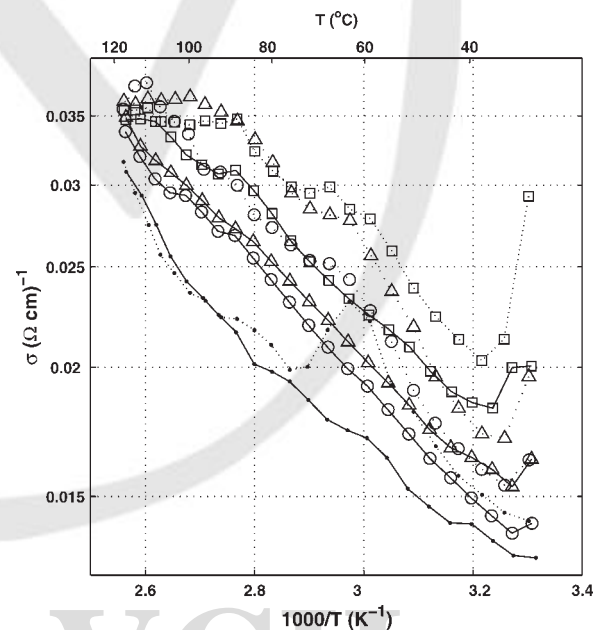


Figure 7.  $\sigma(T)$  values for nc-Si:H films deposited at  $T_s = 175^\circ\text{C}$  on PA, during four cycles within the temperature range: ( $40^\circ\text{C} < T < 120^\circ\text{C}$ ).

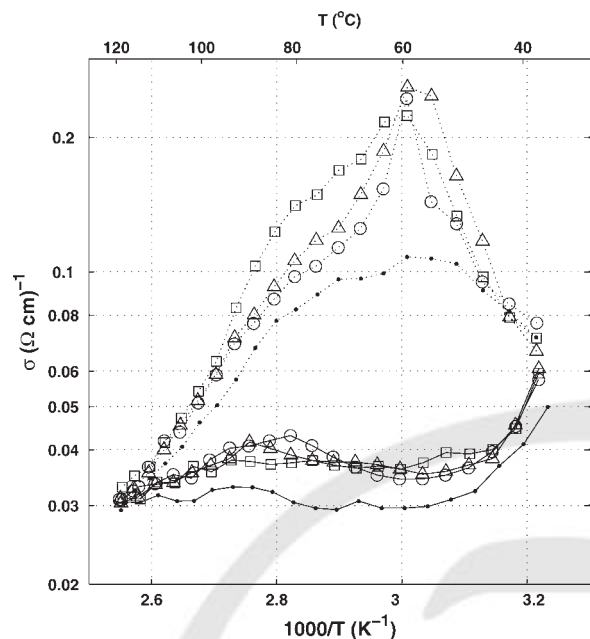


Figure 8.  $\sigma(T)$  values for nc-Si:H films deposited at  $T_s = 175^\circ\text{C}$  on PO, during four cycles through the temperature range: ( $40^\circ\text{C} < T < 120^\circ\text{C}$ ).

stress values in the nc-Si:H deposits on this substrate increase concomitantly with rising  $T$ , and this gives rise to the hysteretic, non-Arrhenius behavior observed in Figure 8. For the case of all other substrate materials,  $\alpha$  is either constant or only mildly  $T$ -dependent (see Figure 2 and Table 1) so that this “anomaly” does not occur. The series of near-parallel linear curves in Figure 7, which eventually stabilize to a single, reproducible one, result from gradual relaxation of the residual stresses in the polymer that originate from the manufacturing process.

In Figure 9 we present a series of Arrhenius plots corresponding to different substrate materials (PS, PA, PI and glass), in all cases following mechanical relaxation of possible stresses in the substrates, and all nc-Si:H films having been deposited under identical conditions at  $T_s = 175^\circ\text{C}$ . Clearly, the curves are all parallel ( $E_a = 92 \pm 5$  meV), but the  $\sigma(T')$  values can differ by a factor of about 1.5 for any given  $T'$  value. For easier comparison with data from the literature, we shall focus our attention on our data pertaining to the Corning 2947 glass substrate material: Figure 10 shows plots of  $\sigma(300\text{ K})$ , values measured at 300 K, versus the corresponding apparent  $E_a$  values, along with similar plots drawn from the literature.<sup>[7,20]</sup> Even though the latter correspond to significantly different fabrication conditions (for example, Ram et al.<sup>[7]</sup> used  $\text{SiF}_4$  as their Si feed gas, instead of  $\text{SiH}_4$ ), the three data sets are remarkably similar. Figure 11 and 12 show plots of  $\sigma(300\text{ K})$  and of  $E_a$  values versus  $T_s$  and  $X_c$ , respectively, for the present a-Si:H and nc-Si:H deposits, again on the Corning 2947 glass substrates. Like the data displayed in Figure 10, these illustrate the remarkable range of property variations,

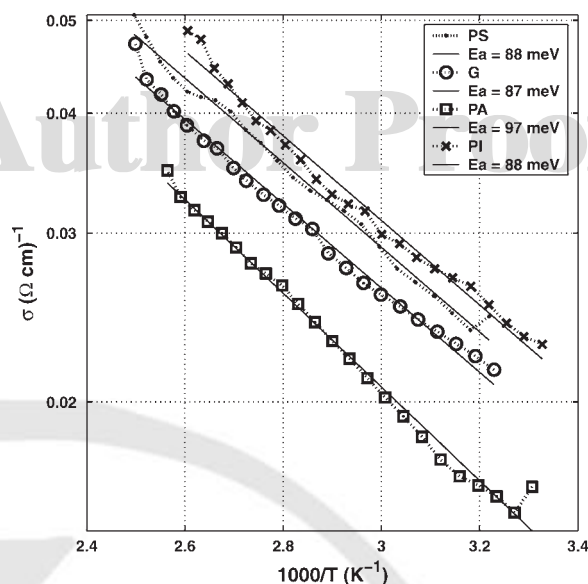


Figure 9. Arrhenius plots for nc-Si:H films on glass and on three polymer substrates, all deposited at  $T_s = 175^\circ\text{C}$ .

their systematic dependence on  $T_s$  (or  $X_c$ , itself strongly dependent on  $T_s$ ), and their excellent reproducibilities achieved in the current research. Although the data are not shown here (other than in the example of Figure 9), similar results were also obtained with the “well-behaved” polymer substrates, that is, all but PO.

As mentioned in connection with Figure 10, the present data correlate well with those in the literature, but only if one takes into account the “normal” existence of oxygen doping of the nc-Si:H at the ppm level. This is

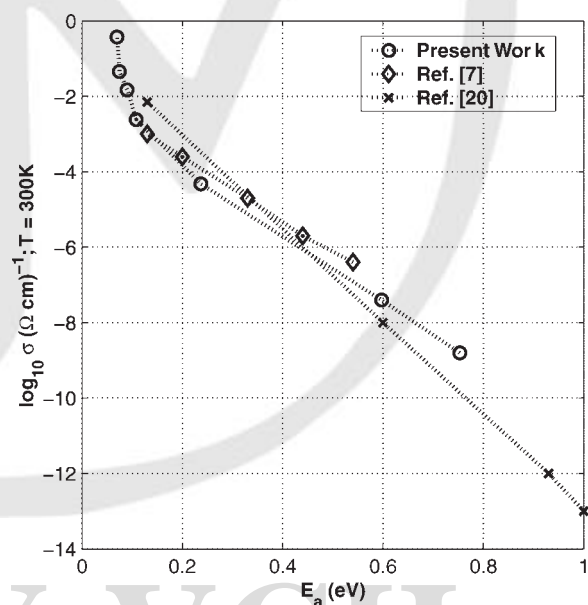


Figure 10. Plots of  $\sigma$  values measured at 300 K versus the corresponding apparent  $E_a$  values, for the present work and data from the literature.<sup>[7,20]</sup>

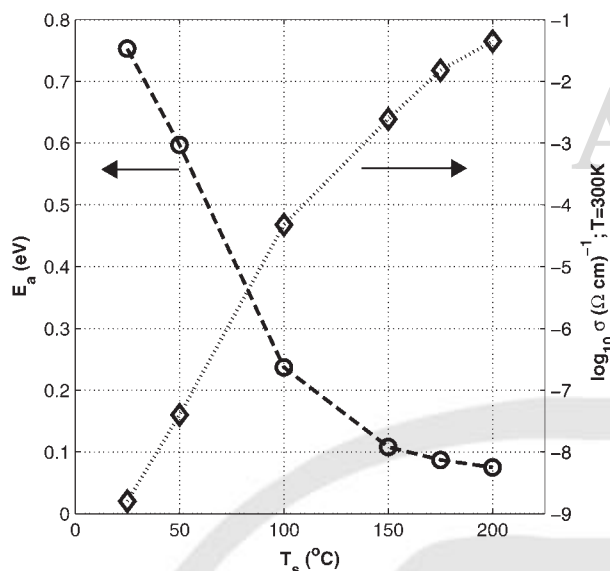


Figure 11. Plots of  $\sigma(300 \text{ K})$  and of  $E_a$  values versus substrate temperature,  $T_s$ , at which the nc-Si:H films were deposited, for the case of Corning 2947 glass substrate material.

known to occur on account of trace quantities of  $\text{O}_2$  and  $\text{H}_2\text{O}$  in the reactor; Torres et al.<sup>[21]</sup> demonstrated that O-doping could only be avoided by taking extraordinary measures for assuring purity of the feed gas and of the reactor system.

## General Discussion and Conclusion

Like the present work, other earlier research<sup>[5–7]</sup> also had an objective to elucidate the structural evolution of thin Si

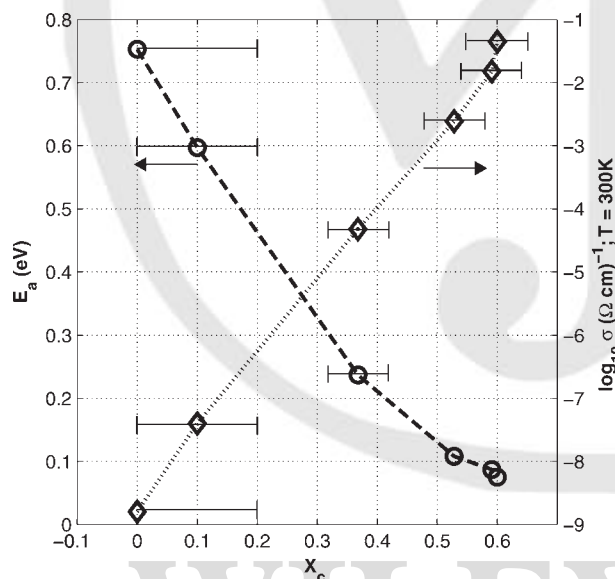


Figure 12. Plots of  $\sigma(300 \text{ K})$  and of  $E_a$  values versus the films' crystalline volume fraction,  $X_c$ , for the case of nc-Si:H films deposited on Corning 2947 glass.

films, deposited by PECVD from  $\text{SiH}_4$  mixtures highly diluted in  $\text{H}_2$ , for the most part using silica or c-Si substrates. With a suitable choice of  $C_{\text{SiH}_4}$  (between 5% and 8%, 6.25% in the present case) it was found that the nanostructure of deposited films can be effectively controlled by varying a single parameter,  $T_s$ .<sup>[5–7]</sup> The present structural and electrical results also clearly demonstrate that a very wide range of material properties can be achieved simply by varying  $T_s$  within the range tolerated by the current substrate materials ( $T_s < 250^\circ \text{C}$ ). The first appearance of nanocrystalline structure (detected by MRS) occurred at  $T_s = 100 \pm 10^\circ \text{C}$  (Figure 6). Thermal expansion of these substrates has clearly been our greatest challenge for the development of highly stable film-substrate composite structures. Compressive strains ( $\alpha_s \Delta T \approx 1.7\%$ ) and compressive stress values  $s_f \approx 3.6 \text{ GPa}$ , have been identified as those that clearly exceeded the adhesive strength of the nc-Si:H/PO interface, when  $T_s \geq 200^\circ \text{C}$ . Although highly stressed samples (PO substrate,  $T_s = 175^\circ \text{C}$ ) were not observed to immediately delaminate, their  $\sigma(T)$  behavior was hysteretic (Figure 8), and they eventually did delaminate after numerous thermal cycles ( $\approx 10$  cycles of  $\approx 8 \text{ h}$  per cycle). The large majority of nc-Si:H films on polymers nevertheless showed resilience, as evidenced by the stability of their electrical behaviors (linear Arrhenius plots for nc-Si:H on all substrates other than PO), even when repeatedly subjected to  $\approx \text{GPa}$  stresses, both in tension and compression, for example during continuous thermal cycling for periods in excess of 80 h. Like Angiolini et al.,<sup>[1]</sup> we are therefore confident that the results presented here “point to the successful fabrication of high-performance TFT arrays on plastic substrates”.

The high- $T_g$  polymers we have used here as substrates fulfill certain important requirements for electronic applications, for example in OLED technology: Their high  $T_g$  values and their resistance to plasma-induced ablation have allowed us to deposit satisfactory nc-Si:H layers by RF-PECVD, subject to the selection of suitable deposition parameters. The high expansion coefficients of some polymers, particularly of PO, remains an important obstacle opposing fabrication of reliable devices, yet the resilience of nc-Si:H films observed on substrates other than PO is encouraging. Relationships between deposition conditions, structural and transport properties that we have observed manifest much similarity between the behaviors of nc-Si:H films grown on glass and on polymer substrates.

**Acknowledgements:** This work is supported by grants from the Natural Sciences and Engineering Research Council of Canada (NSERC). The authors are grateful to Drs. X.-M. Zhao and R. A. Shick of Promerus LLC, for providing high- $T_g$  substrate materials (PO, PA, and PS) and for valuable discussions. We also thank the staff at the LMF and LCM laboratories at *École Polytechnique* and at the *Université de Montréal* for valuable assistance.

- [1] S. Angiolini, M. Avidano, R. Bracco, C. Barlocco, N. D. Young, M. Trainor, X.-M. Zhao, *SID Digest* **2003**, 47.1.
- [2] Anon, "see what can be high performance films"; pamphlet published jointly by Ferrania Imaging Technologies, Promeris LLC and Sumitomo Bakelite Co., Ltd.
- [3] "Thin Film Transistors", Y. Kuo, Ed., Kluwer Academic Publishers, Dordrecht 2004.
- [4] *SOI Design: Analog, Memory and Digital Techniques*, A. Marshall, S. Natarajan, Eds., Kluwer Academic Publishers, Dordrecht 2002.
- [5] U. Kroll, J. Meier, A. Shah, S. Mikhailov, J. Weber, *J. Appl. Phys.* **1996**, *80*, 4971.
- [6] O. Vetterl, A. Gross, T. Jana, S. Ray, A. Lambert, R. Carius, F. Finger, *J. Non-Cryst. Sol.* **2003**, 299–302, 772.
- [7] S. K. Ram, S. Kumar, R. Vanderhagen, P. Roca, I. Cabarrocas, *J. Non-Cryst. Sol.* **2002**, 299–302, 411.
- [8] Z. Suo, E. Y. Ma, H. Gleskova, S. Wagner, *Appl. Phys. Lett.* **1999**, *74*, 1177.
- [9] H. Gleskova, S. Wagner, Z. Suo, *Appl. Phys. Lett.* **1999**, *75*, 3011.
- [10] M. Ohring, "Material Science of Thin Films", 2<sup>nd</sup> edition, Academic Press, Boca Raton 2002.
- [11] E. Bustarret, M. A. Hachicha, M. Brunel, *Appl. Phys. Lett.* **1988**, *52*, 1675.
- [12] G. Yue, J. D. Lorentzen, J. Lin, D. Han, Q. Wang, *Appl. Phys. Lett.* **1999**, *75*, 492.
- [13] C. Droz, E. Vallet-Sauvain, J. Bailat, L. Feitknecht, J. Meier, A. Shah, *Solar Energy Mater. Solar Cells* **2004**, *81*, 61.
- [14] I. H. Campbell, P. M. Fauchet, *Solid State Commun.* **1986**, *58*, 739.
- [15] D. M. Bhusari, A. S. Kumbhar, S. T. Kshirsagar, *Phys. Rev. B* **1993**, *47*, 6460.
- [16] V. Paillard, P. Puech, P. Roca, I. Cabarrocas, *J. Non-Cryst. Sol.* **2002**, 299–302, 280.
- [17] J. Owen, D. Han, B. Yan, J. Yang, K. Lord, S. Guha, *NCPV and Solar Review Meeting*, 2003, NREL/CD-520-33586, 776.
- [18] F. M. Smits, *Bell Syst. Tech. J.* **1958**, 37.3.
- [19] D. M. Manos, D. L. Flamm, "Plasma Etching: An Introduction", Academic Press, Boston 1988.
- [20] R. Platz, S. Wagner, *J. Vac. Sci. Technol. A* **1988**, *16*, 3218.
- [21] P. Torres, J. Meier, R. Fluckinger, U. Kroll, J. A. Anna Selvan, H. Keppner, A. Shah, S. D. Littelwood, I. E. Kelly, P. Giannoules, *Appl. Phys. Lett.* **1996**, *69*, 1373.

**Q1:** Please check Figure 6, 7, and 8, e-file and hardcopy mismatch.

WILEY-VCH